Hindawi Publishing Corporation
EURASIP Journal on Wireless Communications and Networking
Volume 2010, Article ID 659291, 8 pages
doi:10.1155/2010/659291

Research Article

The Performance of Network Coding at the Physical Layer with Imperfect Self-Information Removal

Haris Gacanin and Fumiyuki Adachi

Department of Electrical and Communication Engineering, Graduate School of Engineering, Tohoku University, 6-6-05 Aza-Aoba, Aramaki, Aoba-ku, Sendai 980-8579, Japan

Correspondence should be addressed to Haris Gacanin, harisg@ieee.org

Received 30 December 2009; Revised 14 April 2010; Accepted 8 July 2010

Academic Editor: Petar Popovski

Network capacity for bidirectional communication between pairs of wireless end users assisted by a relay terminal can be improved by network coding at the physical layer (PNC). Narrowband analog network coding (ANC) was introduced as a simpler implementation of PNC in a flat (i.e., frequency-nonselective fading) channel. Recently, broadband ANC has been studied for communication over a frequency-selective fading channel. In ANC, the end user removes its own information from the received signal before detecting the data of the other user. Clearly, the network performance of ANC scheme depends on the self-information removal at the destination terminal. In this paper, we discuss the impact of imperfect self-information removal on the performance of broadband ANC in terms of the bit error rate (BER) and achievable throughput in a frequency-selective fading channel. The theoretical minimum mean square error (MMSE) equalization weight for ANC based on single carrier with frequency domain equalization (SC-FDE) radio access is derived by taking into account the self-interference. We have used analysis and computer simulation to evaluate how the imperfect removal of self-information influences the achievable BER and throughput.

1. Introduction

Next generation wireless communication networks are expected to provide gigabit ubiquitous access and coverage over a large area for wireless users. To enable gigabit broadband services for wireless end-users, a higher capacity is required. Direct application of network coding [1] in a wireless relaying [2] at the physical layer increases the capacity of bi-directional communication in a flat (i.e., frequency-nonselective) fading channel (called bi-directional amplification of the throughput (BAT-relaying) in [3] and physical layer network coding (PNC) in [4]). The analog network coding (ANC) proposed in [5] is essentially another variation of BAT-relaying and PNC schemes in a flat fading channel with a simpler implementation. Recently, broadband ANC based on orthogonal frequency division multiplexing (OFDM) and single carrier with frequency domain equalization (SC-FDE) was investigated in a multipath (i.e., frequency-selective) fading channel [6].

In the ANC scheme, communication is done in two stages; in the first stage both users transmit their signals to the relay, while in the second stage the relay broadcasts the received signal. At the destination terminal, the self-information is removed from the received signal before data detection. Naturally the network performance of ANC scheme highly depends on the self-information removal at the destination terminal. Self-information removal accuracy can be degraded due to several factors such as imperfect frame synchronization, carrier frequency offset, and imperfect knowledge of channel state information. Early studies [3–6] considered perfect self-information removal at the destination terminal. Therefore, an important question is "How much does the imperfect self-information removal affect the performance of ANC scheme?" To the best of authors knowledge, this effect has not been evaluated in the literature yet.

This paper investigates the performance of bi-directional ANC with imperfect self-information removal based on OFDM and SC-FDE radio access in a frequency-selective

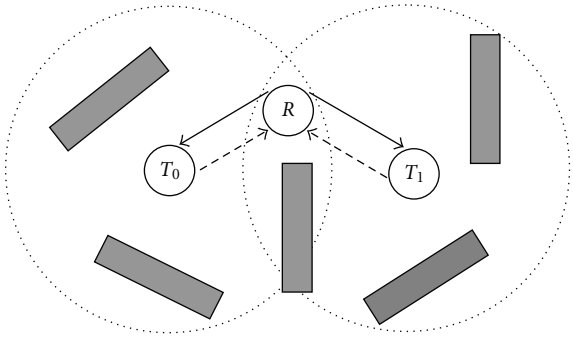

Figure 1: Network model.

fading channel. The performance metrics of practical interest are (i) the bit error rate (BER) and (ii) throughput. The achievable performance with imperfect self-information removal is evaluated by analysis and computer simulation. We develop a theoretical model to take into consideration a random nature of self-interference due to imperfect self-information removal. The theoretical MMSE weight for SC-FDE is derived by taking into account the self-interference. The theoretical expressions are derived based on the Gaussian approximation of both the residual inter-symbol interference (ISI) after equalization and the self-interference due to imperfect self-information removal.

The remainder of this paper is organized as follows. Section 2 explains the network model. In Section 3, we present the theoretical performance with imperfect self-information removal. Numerical and computer simulation results are presented in Section 4. Section 5 concludes the paper.

2. Network Model

This section firstly presents bi-directional ANC based on OFDM and SC-FDE radio access, and then we present a theoretical model for random self-interference due to imperfect self-information removal.

2.1. Broadband ANC Scheme. A two-way relay network with the users T_0 and T_1 and the relay R is illustrated in Figure 1. We assume that coverage area of terminals T_0 and T_1 includes relay terminal R while they are out of each other's transmission range due to solid obstacles as illustrated in Figure 1. Each terminal is equipped with an omnidirectional antenna, and the communication takes place in two stages as summarized in Table 1. During the first stage, terminals T_0 and T_1 transmit simultaneously. During the second stage, the relay broadcast the received signal to both terminals T_0 and T_1 using an amplify-and-forward network protocol [7].

Information bit sequence of length M is channel coded, bit interleaved, and mapped into the data-modulated symbols using quadrature phase-shift keying (QPSK) modulation scheme. The terminal T_j data-modulated sequence is divided into N_c-symbol blocks $\{d_j^k(n); n = 0 \sim N_c - 1\}$ for $k = 0 \sim M/N_c - 1$ with $E[|d_j^k(n)|^2]$=1, where $E[\cdot]$ denotes the ensemble average. Henceforth, the frame index k is omitted without loss of generality. We consider two radio access schemes for bi-directional ANC: (i) OFDM and (ii) SC-FDE. In the case of SC radio access, the transmit signal is given by $\{d_j(n)\}$, while in the case of OFDM signaling, $\{d_j(n)\}$ is fed to an N_c-point inverse fast Fourier transform (IFFT) to generate the OFDM signal. After insertion of N_g-sample cyclic prefix into the guard interval (GI), the signal is transmitted over a frequency-selective fading channel.

Table 1: Network protocol.

First stage	Second stage
$T_0, T_1 \rightarrow R$	$R \rightarrow T_0, T_1$

The signal propagates through the channel with a discrete-time channel impulse response $h_{m,j}(\tau)$ given by

$$h_{m,j}(\tau) = \sum_{l=0}^{L-1} h_{l,m,j}\delta(\tau - \tau_l), \tag{1}$$

where L, $h_{l,m,j}$, τ_l, and $\delta(t)$ denote the number of paths, the path gain between the terminal T_j and relay at stage m (=1,2), the lth path time delay normalized by IFFT sampling period, and the delta function, respectively. Without loss of generality, we assume that $\tau_0 = 0 < \tau_1 < \cdots < \tau_{L-1}$ and that the lth path time delay is $\tau_l = l\Delta$, where Δ (≥ 1) defines the separation between adjacent paths.

Stage I. The signals transmitted from both terminals are superimposed in the wireless channel and reach the relay simultaneously. In this paper, we assume ideal synchronization and also assume no path loss and shadowing loss. It should be noted that the assumptions of no path loss and shadowing loss do not change our general conclusion.

The signal received at the relay terminal in the frequency domain can be represented as

$$R_r(n) = \begin{cases} \sqrt{P_s}\left[S_0(n)H_{0,0}(n) + S_1(n)H_{0,1}(n)\right] + N_r(n), & \text{SC}, \\ \sqrt{P_s}\left[d_0(n)H_{0,0}(n) + d_1(n)H_{0,1}(n)\right] + N_r(n), & \text{OFDM}, \end{cases} \tag{2}$$

for $n = 0 \sim N_c - 1$, where P_s (=E_s/T_c), $S_j(n)$, $H_{0,j}(n)$, and $N_r(n)$, respectively, denote the transmit signal power, the Fourier transforms of the terminal T_j transmit signal, the channel gain between T_j and R, and the additive white Gaussian noise (AWGN) at the relay with power spectral density N_0. E_s and T_c denote the data-modulated symbol energy and the sampling interval of IFFT. The received signal at the relay is amplified and broadcasted to both destination terminals.

Stage II. At the terminal T_j, N_c-point FFT is applied to decompose the received signal into N_c frequency components represented by

$$R_j(n) = \sqrt{P_s}R_r(n)H_{1,j}(n) + N_j(n), \tag{3}$$

for $j \in \{0, 1\}$ and $n = 0 \sim N_c - 1$, where $R_r(n)$, $H_{1,j}(n)$, and $N_j(n)$ denote the Fourier transforms of the relay transmitted signal, the channel gain between R and terminal T_j, and the additive white Gaussian noise (AWGN) with power spectral density N_0 at the terminal T_j, respectively.

2.2. Self-Information Removal. The terminal T_j removes its self-information from the received signal. However, the self-information removal is not perfect, and hence, the self interference is present. Since an exact analysis of self interference is quite difficult if not impossible, we introduce a simplified model to include the random interference resulting from, for example, imperfect channel estimation as

$$\widetilde{R}_j(n) = R_j(n) - P_s S_j(n) \widehat{H}_{0,j}(n) \widehat{H}_{1,j}(n), \tag{4}$$

where $S_j(n)$ denotes the SC- or OFDM-transmitted signal of the terminal T_j (i.e., $\{d_j(n)\}$ in case of OFDM and FFT$[\{d_j(n)\}]$ for SC-FDE). In (4), $\widehat{H}_{m,j}(n) = H_{m,j}(n) - \delta_{m,j}(n)$, where the error term $\delta_{m,j}(n)$ $(m = 0, 1)$ is assumed to be independent zero mean complex Gaussian random variable [8]. Thus, we can rewrite (4) as

$$\widetilde{R}_j(n) = R_j(n) - P_s S_j(n) H_{0,j}(n) H_{1,j}(n) + \Delta_j(n), \tag{5}$$

where $\Delta_j(n)$ denotes the random self interference due to imperfect channel estimation given by

$$\begin{aligned} \Delta_j(n) = P_s \Big[& H_{0,j}(n)\delta_{1,j}(n) + H_{1,j}(n)\delta_{0,j}(n) \\ & + \delta_{0,j}(n)\delta_{1,j}(n) \Big]. \end{aligned} \tag{6}$$

For the given channel gains $H_{m,j}(n)$, the products $H_{1,j}(n)\delta_{0,j}(n)$ and $H_{1,j}(n)\delta_{0,j}(n)$ are also assumed to be independent complex Gaussian random variables. On the other hand, the cross term $\delta_{0,j}(n)\delta_{1,j}(n)$ is not a Gaussian variable. However, most of the time, the term $\delta_{0,j}(n)\delta_{1,j}(n)$ is much smaller than $H_{1,j}(n)\delta_{0,j}(n) + H_{1,j}(n)\delta_{0,j}(n)$ and therefore can be neglected. As a consequence, the self interference $\Delta_j(n)$ behaves as a complex Gaussian random variable with the variance given as $E[|\Delta_j(n)|^2] = P_s^2 \beta^2 \overline{H}(n)$, where $\overline{H}(n) = |H_{0,j}(n)|^2 + |H_{1,j}(n)|^2$ and $\beta = \sqrt{E[|\delta_{m,j}(n)|^2]}$ denotes the root mean square (rms) estimation error, which reflects the degree of imperfect self-information removal due to estimation error at the destination end. The case with $\beta = 0$ represents the perfect self-information removal case. We note here that the self interference also may be caused by imperfect synchronization, carrier frequency offset, and so forth, in addition to the imperfect channel estimation, but their analysis is out of the scope of this work.

2.3. FDE. One-tap equalization is applied in the frequency domain to combat the channel impairments as presented below. The equalized signal can be represented as

$$\widehat{R}_j(n) = \widetilde{R}_j(n) w_j(n), \tag{7}$$

for $n = 0 \sim N_c - 1$, where the equalization weight at the terminal T_j is given by (8) at the top of the next page. We note here that the theoretical MMSE equalization weight for SC-FDE is derived to take into consideration the random interference due to imperfect self-information removal (see the appendix).

$$w_j(n) = \begin{cases} \dfrac{H^*_{0,\bar{j}}(n) H^*_{1,j}(n)}{\left|H_{0,\bar{j}}(n) H_{1,j}(n)\right|^2 + \beta^2 \overline{H}(n) + (E_s/2N_0)^{-1} \left|H_{1,j}(n)\right|^2 + (E_s/2N_0)^{-2}}, & \text{SC}, \\ \dfrac{H^*_{0,\bar{j}}(n) H^*_{1,j}(n)}{\left|H_{0,\bar{j}}(n) H_{1,j}(n)\right|^2}, & \text{OFDM}. \end{cases} \tag{8}$$

In the case of SC-FDE transmission, N_c-point IFFT is applied to (7) to obtain decision variables for data detection, while for OFDM case, (7) denotes the decision variables. Finally, the log-likelihood ratio (LLR) is computed, and de-interleaving followed by Viterbi decoding is carried out.

3. Performance Analysis

In this section, we first present the conditional signal-to-interference plus noise ratio (SINR) taking into account imperfect self-information removal. Later the conditional BER and throughput expressions are presented. We note here that the derivation of closed form BER and throughput expressions with imperfect self-information removal is very difficult if not impossible due to the presence of the residual ISI after FDE and self interference term in (11). We assume that the relay normalizes received signal (2) by the factor α which represents its noise variance. This will not alter the signal-to-noise ratio (SNR) but will assist theoretical derivations.

3.1. Decision Variables with Imperfect Self-Information Removal. Using (2) through (6), the decision variables at the terminal T_j after equalization can be expressed as

$$\widehat{d}_j(n) = \begin{cases} P_s d_{\bar{j}}(n) \widetilde{H} + I_j(n) + \dfrac{1}{N_c} \displaystyle\sum_{n=0}^{N_c-1} \widetilde{N}_j(n), & \text{SC}, \\ P_s d_{\bar{j}}(n) \widehat{H}_j(n) + I_j(n) + \widetilde{N}_j(n), & \text{OFDM}, \end{cases} \tag{9}$$

where

$$\widetilde{H} = \frac{1}{\sqrt{\alpha}}\frac{1}{N_c}\sum_{n=0}^{N_c-1} H_{0,\bar{j}}(n)H_{1,j}(n)w_j(n),$$
$$\widehat{H}_j(n) = \frac{1}{\sqrt{\alpha}}H_{0,\bar{j}}(n)H_{1,j}(n)w_j(n), \quad (10)$$
$$\widetilde{N}_j = \frac{P_s}{\sqrt{\alpha}}H_{1,j}(n)N_r(n)w_j(n) + N_j(n)w_j(n),$$

with $\bar{j} = 0(1)$ if $j = 1(0)$. In (9), $S_j(n) = d_j(n)$ in the case of OFDM while $S_j(n) = \mathrm{FFT}[\{d_j(n)\}]$ for SC-FDE radio access. $I_j(n)$ denotes the total interference (i.e., the residual ISI after equalization plus random self interference due to imperfect self-information removal) given by (11) at the top of the next page. We note here that in the case of OFDM the ISI is eliminated by the insertion of the cyclic prefix within the GI.

$$I_j(n) = \begin{cases} \dfrac{P_s}{\sqrt{\alpha}N_c}\displaystyle\sum_{n=0}^{N_c-1}\widehat{H}(n)\sum_{t'=0}^{N_c-1} d_{\bar{j}}(t')\exp\left(j2\pi n\frac{t-t'}{N_c}\right) \\ \qquad + \dfrac{1}{\sqrt{\alpha}N_c}\displaystyle\sum_{n=0}^{N_c-1}\Delta_j(n)w_j(n), & \text{SC}, \\ \dfrac{1}{\sqrt{\alpha}}\Delta_j(n)w_j(n), & \text{OFDM}. \end{cases} \quad (11)$$

It can be seen from (11) that the residual ISI is a weighted sum of a large number of independent and identically distributed (i.i.d.) data-modulated symbols as shown by summation in (11). The Gaussian approximation of the residual ISI remains valid only if the number of ISI components is large and if they are i.i.d. so that the central limit theorem can be considered. This is true for OFDM and SC-FDE when the IFFT/FFT size is large enough. Thus, we assume that the residual ISI after FDE, for SC-FDE, can be approximated as a complex-valued random Gaussian variable. Consequently, since the self interference due to imperfect self-information removal can be approximated as a complex-valued random Gaussian variable (see Section 2.2), the sum of the residual ISI, the self interference, and AWGN can be treated as a new complex-valued random Gaussian noise with variance $2\sigma^2$ given by

$$2\sigma^2 = \begin{cases} \dfrac{2N_0}{T_cN_c}\dfrac{1}{N_c}\displaystyle\sum_{n=0}^{N_c-1}\left|w_j(n)\right|^2 \\ \quad + \dfrac{2N_0}{T_cN_c}\dfrac{P_s}{\alpha N_c}\displaystyle\sum_{n=0}^{N_c-1}\left|H_{1,j}(n)w_j(n)\right|^2 \\ \quad + \dfrac{P_s^2}{\alpha N_c}\displaystyle\sum_{n=0}^{N_c-1}\left|\widehat{H}_j(n)w_j(n)\right|^2 - \left|\widetilde{H}\right|^2 \\ \quad + \dfrac{\beta^2P_s^2}{\alpha N_c}\displaystyle\sum_{n=0}^{N_c-1}\overline{H}(n)\left|w_j(n)\right|^2, & \text{SC}, \\ \dfrac{2N_0}{T_cN_c}\left|w_j(n)\right|^2 \\ \quad + \dfrac{2N_0}{T_cN_c}\dfrac{P_s}{\alpha}\left|H_{1,j}(n)w_j(n)\right|^2 \\ \quad + \dfrac{\beta^2P_s^2}{\alpha}\overline{H}(n)\left|w_j(n)\right|^2, & \text{OFDM}. \end{cases} \quad (12)$$

It can be seen from (9) that the OFDM (SC-FDE) equalized (IFFT) output can be seen as a random variable with mean $P_sd_{\bar{j}}(n)\widehat{H}$ ($P_sd_{\bar{j}}(n)\widetilde{H}(n)$). Using (9) and (12), the conditional signal-to-interference plus noise ratio (SINR) $\gamma_j[E_s/N_0, \{H_{m,j}(n)\}]$ at the jth terminal T_j is represented by (13).

$$\gamma_j\left[\frac{E_s}{N_0}, \left\{H_{m,j}(n)\right\}\right] = \begin{cases} \dfrac{\left|\widetilde{H}\right|^2}{\left(\frac{1}{N_c}\right)\sum_{n=0}^{N_c-1}\left|\widehat{H}\right|^2 - \left|\widetilde{H}\right|^2 + \left(\frac{\beta}{N_c}\right)^2\sum_{n=0}^{N_c-1}\overline{H}(n)\left|w_j(n)\right|^2 + \left(\frac{1}{N_c}\right)\sum_{n=0}^{N_c-1}\left[\left(\frac{E_sN_c}{2N_0}\right)^{-1}\left|H_{1,j}(n)\right|^2 + \left(\frac{E_s}{2N_0}\right)^{-2}\right]\left|w_j(n)\right|^2}, & \text{SC}, \\ \dfrac{\left|H_{0,\bar{j}}(n)\right|^2\left|H_{1,j}(n)\right|^2}{\beta^2\overline{H}(n) + \left(\frac{E_s}{2N_0}\right)^{-1}\left|H_{1,j}(n)\right|^2 + \left(\frac{E_s}{2N_0}\right)^{-2}}, & \text{OFDM}. \end{cases} \quad (13)$$

3.2. BER and Throughput Analysis for Uncoded System. We assume QPSK data modulation with all "1" transmission without loss of generality. The conditional BER at the terminal T_j is given by [8]

$$P_{j,b}\left(\frac{E_s}{N_0}, \left\{H_{m,j}(n)\right\}\right) = \frac{1}{2}\,\mathrm{erfc}\left[\sqrt{\frac{1}{4}\gamma_j\left(\frac{E_s}{N_0}, \left\{H_{m,j}(n)\right\}\right)}\right], \quad (14)$$

where E_s/N_0 and $\mathrm{erfc}[\cdot]$ denote the given average signal energy per symbol-to-AWGN power spectrum density ratio and the complementary error function, respectively. We define the packet length of M bits. Using (14), the conditional packet error rate (PER) at the terminal T_j can be expressed by

$$P_{j,\mathrm{packet}}\left(\frac{E_s}{N_0}, \left\{H_{m,j}(n)\right\}\right) = 1 - \left[1 - P_{j,b}\left(\frac{E_s}{N_0}, \left\{H_{m,j}(n)\right\}\right)\right]^M. \quad (15)$$

The average PER at terminal T_j can be numerically evaluated by averaging the conditional PER (15) over all possible

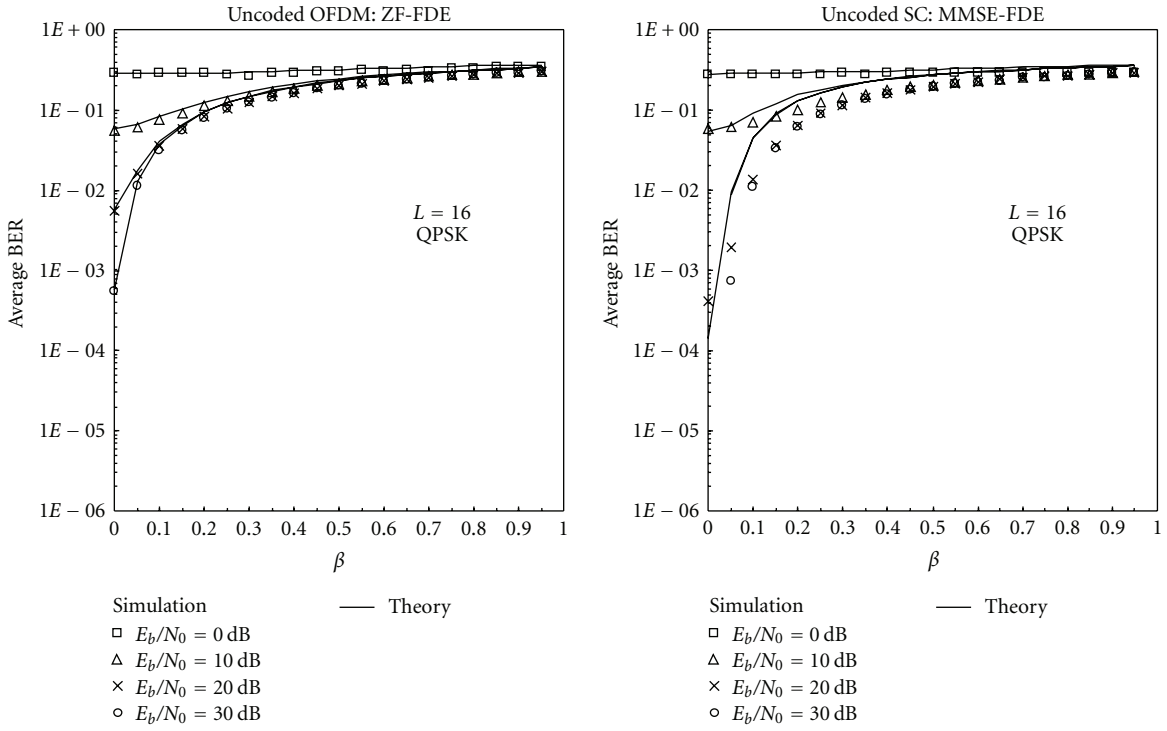

(a) OFDM radio access

(b) SC-FDE radio access

Figure 2: Uncoded BER versus β of broadband ANC.

realizations of $\{H_{m,j}(n);\ n = 0 \sim N_c - 1\}$ as

$$P_{j,\text{packet}}\left(\frac{E_s}{N_0}\right) = E\left[P_{j,\text{packet}}\left(\frac{E_s}{N_0}, \left\{H_{m,j}(n)\right\}\right)\right]. \tag{16}$$

Finally, the achievable throughput η_j at terminal T_j is given as

$$\eta_j = 1 - P_{j,\text{packet}}\left(\frac{E_s}{N_0}\right), \tag{17}$$

which is the theoretical throughput achievable by selective repeat ARQ, where the transmission is done using a packet of 2 OFDM symbols (i.e., two N_c-sample IFFT blocks).

The evaluation of the throughput is done by Monte-Carlo numerical computation method as follows. First, a set of channel gains $\{H_{m,j}(n);\ n = 0 \sim N_c - 1\}$ is generated as a Fourier transform of the corresponding channel impulse response given by (1). Then, the equalization weight $\{w_j(n);\ n = 0 \sim N_c - 1\}$ is computed for each of the source terminals [6]. Secondly, the conditional BER is computed using (14) for the given set of channel gains $\{H_{m,j}(n)\}$ for the given E_s/N_0. Then, the average PER is computed using (16) to obtain the achievable throughput by evaluating (17).

4. Results and Discussions

Numerical and computer simulation parameters are summarized in Table 2. In our numerical evaluation and computer simulation, we assume $N_c = 256$, GI length of $N_g = 32$ samples, and ideal coherent QPSK data modulation and demodulation. The information bit sequence length is taken to be 1024 bits. For channel coding, we apply $\{g_1 = (111), g_2 = (101)\}$ convolutional encoder [9] with coding rate 1/2 and constraint length 3 (each new frame state of the encoder is initialized before transmission). 2048-bit random interleaver is used as channel interleaver. At the receiver, a hard decision Viterbi decoder is applied. The propagation channel is an $L = 16$-path block Rayleigh fading channel having the uniform power delay profile, where $\{h_{l,m,j};\ l = 0 \sim L - 1\}$ are zero mean independent complex variables with $E[|h_{l,m,j}|^2] = 1/L$. The normalized Doppler frequency $f_D T_s = 10^{-4}$, where $1/T_s = 1/[T_c(1 + N_g/N_c)]$ is the transmission symbol rate, is assumed (under this assumption, the path gains can be considered to remain almost constant over a packet of 1024 information bits and vary packet-by-packet). We assume that the maximum time delay of the channel is less than the GI length (i.e., $L < N_g$ with $\Delta = 1$) and that all paths in any channel are independent of each other. In this paper, we do not consider geometry, and thus, we assume neither shadowing nor path loss.

4.1. BER. We perform computer simulation to evaluate the uncoded and coded BER of broadband ANC as a function of the cancelation factor β with the average signal energy per bit-to-AWGN power spectrum density ratio E_b/N_0 $(= 0.5 \times 0.5 \times (E_s/N_0) \times (1 + N_g/N_c))$ as a parameter being illustrated in Figures 2 and 3. The uncoded BER is evaluated by both numerical computation using (14) and computer simulation, while the coded BER is measured by computer simulation.

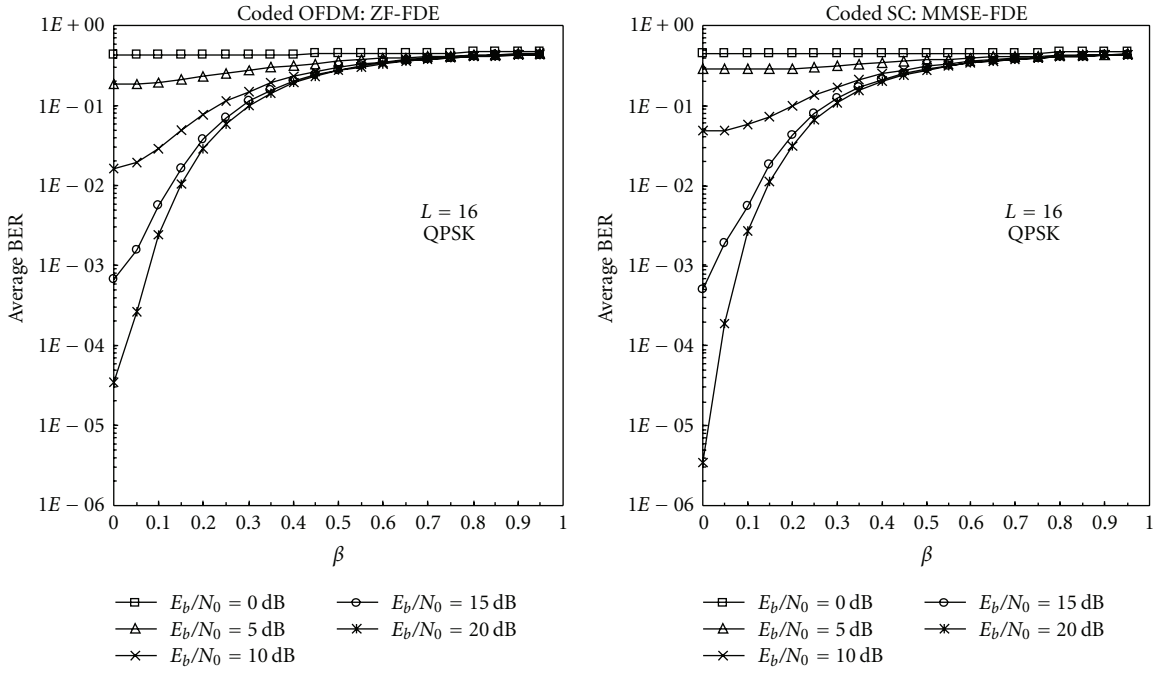

(a) OFDM radio access (b) SC-FDE radio access

Figure 3: Coded BER versus β.

Table 2: Simulation parameters.

Transmitter	Data modulation	QPSK
	Block/IFFT size	N_c=256
	GI	$N_g = 32$
Channel	L-path block Rayleigh fading with $\Delta = 1$	
Receiver	FDE	MMSE, ZF
	Channel estimation	Ideal

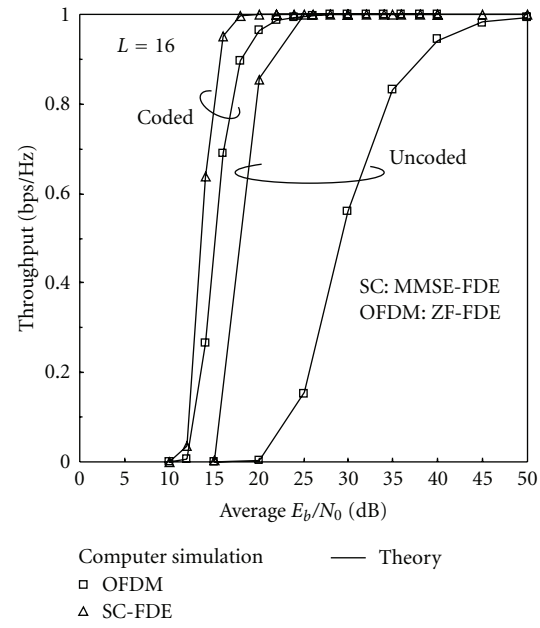

Figure 4: Throughput versus E_b/N_0.

It can be seen from the figure that in a lower E_b/N_0 region, impact of imperfect self-information removal is negligible; for $E_b/N_0 = 0$ and 5 dB, the BER performance slightly degrades as the cancelation coefficient β increases. On the other side, for a higher E_b/N_0, the BER performance is severely affected by imperfect self-information removal. For example, if 10 times increase of the BER performance is allowable in comparison with the perfect self-information removal (i.e., $\beta = 0$) case, it is required to cancel 96% of self-information ($\beta = 0.04$ in Figure 2) for uncoded OFDM case, while SC-FDE radio access is more sensitive to self-information removal since more than 99% of cancelation is required to allow only 10 times performance degradation. It can be seen from the figure that more self-interference is allowed in the lower E_b/N_0 region to achieve the same performance degradation.

In the case of channel coding illustrated in Figure 3, a higher resistance to imperfect self-information removal due to channel coding gain is observed; a lower percentage of cancelation is required to allow 10 times performance degradation in comparison with the uncoded case. Note that, the BER of broadband ANC based on SC-FDE is lower in comparison with OFDM radio access due to the frequency diversity gain obtained through MMSE-FDE. However, the BER performance between their coded performances is significantly reduced since OFDM system achieves the frequency diversity gain through channel decoding. In this paper, we assume simple convolutional encoding and hard

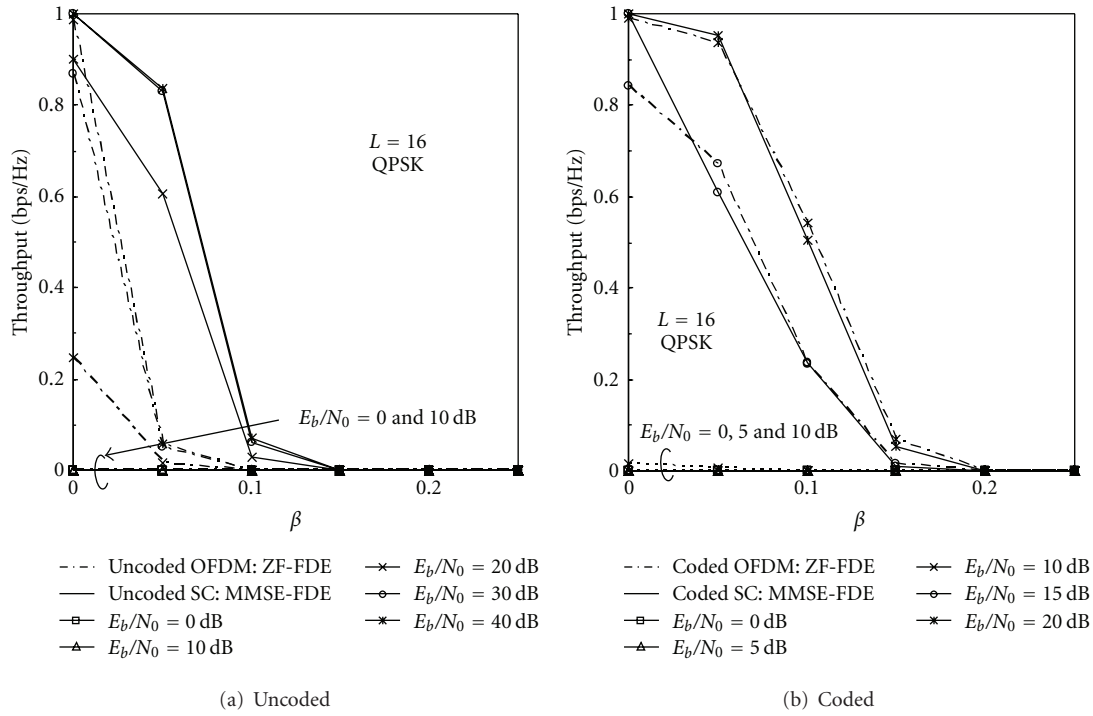

Figure 5: Throughput versus β.

decision Viterbi decoding, which provides a relatively small coding gain. Much larger coding gain can be obtained with soft decision decoding or state-of-the-art channel coding techniques such as turbo codes and low-density parity check codes.

4.2. Throughput. The achievable throughput of broadband ANC as a function of E_b/N_0 is illustrated in Figure 5 for (i) uncoded and (ii) coded cases. The uncoded case is numerically evaluated by (17). Throughput in the coded case is evaluated by measuring the BER by computer simulation. Then, the PER is computed using (16) assuming that the bit errors after decoding are random, and finally, we compute the throughput using (17). In the uncoded case, the achievable throughput of broadband ANC using SC-FDE is higher than that using OFDM. This is because SC-FDE is able to exploit the channel frequency selectivity and obtain frequency diversity gain. However, the OFDM system achieves the frequency diversity gain through channel decoding. The performance difference between coded SC-FDE and coded OFDM is significantly reduced. In this paper, we assumed the hard decision decoding; however, the use of soft decision decoding provides better throughput.

Next, we discuss the impact of self-information removal on the achievable throughput. We perform computer simulation to evaluate the achievable throughput of broadband ANC as a function of the cancelation factor β as illustrated in Figure 5. It can be seen from the figure that channel coding provides a better resistance to imperfect self-information removal in comparison with the uncoded case.

5. Conclusion

In this paper, we discussed the impact of imperfect self-information removal on the BER and achievable throughput of bi-directional ANC based on OFDM and SC-FDE radio access in a frequency-selective fading channel. The performance is evaluated by analysis and computer simulation. The theoretical MMSE equalization weight for SC-FDE is derived by taking into account the self interference due to imperfect self-information removal. Our results show that the allowable performance degradation in comparison with the perfect self-information removal case highly depends on the level of E_b/N_0 for both uncoded and coded performances. In the case of channel coding, due to coding gain, a lower percentage of self-information cancelation is required to allow the same performance degradation in comparison with uncoded case. It was also shown that broadband ANC based on SC-FDE is more sensitive to imperfect self-information removal in comparison with OFDM signaling radio access.

The self interference may be caused by different factors such as imperfect synchronization, carrier frequency offset, in addition to channel estimation error, but the analysis taking into account their full impact on the performance is very difficult. This is left as an interesting future work.

Appendix

The equalization weight for SC-FDE signaling, which takes into consideration the random self interference due to imperfect self-information removal, is chosen to minimize the mean square error (MSE) between $\hat{R}_j(n)$ and $S_{\bar{j}}(n)$ at the

nth frequency as $\mathrm{MSE}_j(n) = E[|e_j(n)|^2] = E[|\hat{R}_j(n) - S_{\bar{j}}(n)|^2]$. Substituting (5) into (7), the $\mathrm{MSE}_j(n)$ term can be expressed as

$$\begin{aligned}\mathrm{MSE}_j(n) = {} & \frac{P_s^2}{\alpha} E\left[S_{\bar{j}}(n)S_{\bar{j}}^*(n')\right]\left|H_{0,\bar{j}}(n)H_{1,j}(n)w_j(n)\right|^2 \\ & + \frac{1}{\alpha}E\left[|\Delta_j(n)^2\right]\left|w_j(n)\right|^2 + E\left[S_{\bar{j}}(n)S_{\bar{j}}^*(n')\right] \\ & + \frac{P_s}{\alpha}E[N_r(n)N_r^*(n')]\left|H_{1,j}w_j(n)\right|^2 \\ & + E\left[N_j(n)N_j^*(n')\right]\left|w_j(n)\right|^2,\end{aligned} \tag{A.1}$$

where $N_r(n)$ and $N_j(n)$ denote the zero mean and independent identically distributed (i.i.d.) complex Gaussian variable with variance $2N_0/T_c$. Since data symbols are independent, that is, $E[d(x)d^*(y)] = \delta(x - y)$, we obtain $E[S_{\bar{j}}(n)S_{\bar{j}}^*(n')] = \delta(n - n')$. After the expectation with respect to the noise and self interference components, we obtain

$$\begin{aligned}\mathrm{MSE}_j(n) = {} & \frac{P_s^2}{\alpha}\left|H_{0,\bar{j}}(n)H_{1,j}(n)w_j(n)\right|^2 \\ & + \frac{\beta^2 P_s^2}{\alpha}\overline{H}(n)\left|w_j(n)\right|^2 + \frac{P_s}{\alpha}\frac{2N_0}{T_c}\left|H_{1,j}w_j(n)\right|^2 \\ & - 2P_s^2\Re\left\{E\left[H_{0,\bar{j}}(n)H_{1,j}(n)w_j(n)\right]\right\} \\ & + \frac{2N_0}{T_c}\left|w_j(n)\right|^2 + P_s^2,\end{aligned} \tag{A.2}$$

where $\overline{H}(n) = |H_{0,j}(n)|^2 + |H_{1,j}(n)|^2$, $P_s = E_s/T_c$ and $\Re\{z\}$ denotes the real part of the complex number z. By solving $\partial\mathrm{MSE}_j(n)/\partial w_j(n) = 0$, we obtain the equalization weight given by (8).

References

[1] R. W. Yeung, "Multilevel diversity coding with distortion," *IEEE Transactions on Information Theory*, vol. 41, no. 2, pp. 412–422, 1995.

[2] R. Ahlswede, N. Cai, S.-Y. R. Li, and R. W. Yeung, "Network information flow," *IEEE Transactions on Information Theory*, vol. 46, no. 4, pp. 1204–1216, 2000.

[3] P. Popovski and H. Yomo, "Bi-directional amplification of throughput in a wireless multi-hop network," in *Proceedings of the 63rd IEEE Vehicular Technology Conference (VTC '06)*, Melbourne, Australia, May 2006.

[4] S. Zhang, S. C. Liew, and P. Lam, "Hot topic: physical-layer network coding," in *Proceedings of the 12th Annual International Conference on Mobile Computing and Networking (MOBICOM '06)*, pp. 358–365, Los Angelos, Calif, USA, September 2006.

[5] S. Katti, S. Gollakota, and D. Katabi, "Embracing wireless interference: analog network coding," in *Proceedings of the ACM SIGCOM Conference on Applications, Technologies, Architectures, and Protocols for Computer Communication*, pp. 397–408, Kyoto, Japan, August 2007.

[6] H. Gacanin and F. Adachi, "Broadband analog network coding," *IEEE Transactions on Wireless Communications*, vol. 9, no. 5, pp. 1577–1583, 2010.

[7] J. N. Laneman, D. N. C. Tse, and G. W. Wornell, "Cooperative diversity in wireless networks: efficient protocols and outage behavior," *IEEE Transactions on Information Theory*, vol. 50, no. 12, pp. 3062–3080, 2004.

[8] J. G. Proakis, *Digital Communications*, McGraw-Hill, New York, NY, USA, 3rd edition, 1995.

[9] S. Lin and D. J. Costello, *Error Control Coding: Fundamentals and Aplications*, Prentice Hall, Upper Saddle River, NJ, USA, 1983.